SSRG International Journal of Electronics and Communication Engineering
ISSN: 2348-8549/ https://doi.org/10.14445/23488549/IJECE-V12I12P112

Volume 12 Issue 12, 147-153, December 2025

Original Article

Modeling and Simulation of p-Silicon and n-Silicon Polycrystalline Piezoresistive Pressure Sensors: A Comparative Study

L. Bobinson Singha[1], Maibam Sanju Meetei[1*]

[1]*Electronics and Communication Engineering, Rajiv Gandhi University, Arunachal Pradesh, India.*

[*]*Corresponding Author : maibamkhuman@gmail.com*

Received: 12 October 2025 Revised: 14 November 2025 Accepted: 13 December 2025 Published: 27 December 2025

Abstract - *This study shows a comparative analysis of p-type and n-type Polycrystalline Silicon (Poly-Si) piezoresistive pressure sensors using COMSOL Multiphysics simulation and analytical modeling. The novelty of this study is to study the sensitivity, polarity, linearity, and output span of the sensors with p-type and n-type poly-Si with a doping concentration of $10^{18}cm^{-3}$. The poly-Si-based piezoresistive sensors change their majority charge carrier mobility when deformation occurs. They are also highly compatible with micromachining processes. Therefore, poly-Si-based piezoresistive sensors are widely used in MEMS applications. The p-type and n-type poly-Si with a concentration of $1\times10^{18}\ cm^{-3}$ is used as the sensing material. The mechanical structure used in this study is a cantilever beam with applied pressure on the top. The material used for the mechanical structure is Silicon (Si). A thin layer of Silicon Dioxide (SiO_2) is used as an insulating sheet between the mechanical structure and the poly-Si piezoresistive sensing layer. In Simulation, the voltage terminal is placed at the clamped side, and the ground is placed at the free end of the poly-Si layer. The analytical result and Simulation results demonstrate that both proposed sensors exhibit a highly linear resistance with applied pressure. The polarity of the sensors is positive for the p-type poly-Si-based sensor, while the polarity of the n-type poly-Si is negative. This opposite polarity is due to the presence of a majority charge carrier. The poly-Si piezoresistive pressure sensors exhibit a negative slope for n-type and a positive slope for p-type for the applied pressures ranging from 0 to 100 kPa. Sensor sensitivity is found to be intensely dependent on factors such as the piezoresistive coefficient, doping concentration, electron/hole mobility, and cantilever dimensions (length, width, and thickness). The sensitivity of the simulated p-type and n-type poly-Si piezoresistive pressure sensors is 7.0 mΩ/kPa and -2.29 mΩ/kPa, respectively. The sensitivity of the analytical for p-type and n-type poly-Si piezoresistive pressure sensors is 8.4 mΩ/kPa and -2.31 mΩ/kPa, respectively.*

Keywords - *Carrier mobility, Polycrystalline, Resistivity, Sensitivity, Stress.*

1. Introduction

With the advancement of the Internet of Things (IoT), the miniaturization of sensors with high sensitivity is significant. This is because a smaller size consumes less power, which increases the lifespan of the power supply. The Micro-ElectroMechanical Systems (MEMS)-based sensors have compact size, low power consumption, and high sensitivity, and are widely used in IoT. The MEMS-based pressure sensors can be categorised based on the technology used. They are piezoelectric, piezoresistive, capacitive, inductive, optical, resonant, and resistive [1].

The piezoresistive pressure sensor is one of the most commonly used pressure sensors. This is because of the ability to directly convert the mechanical stress into electrical resistance. The materials that show piezoresistive effect are divided into four groups. They are semiconductors, ceramics, metals, and polymers [2, 3].

Among these piezoresistive materials, the semiconductor-based piezoresistive material has higher resistivity and is highly compatible with the micromachining fabrication technology. This high resistivity is due to the combined effect of the structural deformation and other factors such as carrier concentration, carrier mobility, granular boundaries, and the piezoresistive coefficient of the material [4, 5]. Various semiconductors can be used as piezoresistive materials.

The silicon-based semiconductor is widely used in MEMS applications due to its high piezoresistive coefficient, compatibility with standard CMOS fabrication processes, and mechanical robustness [6, 7]. The silicon-based piezoresistive materials have four major types. They are n-type single crystal, p-type single crystal, n-type and p-type poly-Si. These silicon-based piezoresistive sensors can be tuned to their electrical properties by varying the doping concentration.

Many studies have been done to explore the piezoresistive behaviour of poly-Si under different doping levels. But a simulation and analytical comparative study for these sensors has not been done. So, there is a lack of direct comparative analysis between proposed sensors under identical cantilever mechanical structures with the same doping conditions. This gap limits the understanding of how the majority carrier type, like holes and electrons, influences the sensitivity, polarity, and output span applied pressure.

In the present work, a comparative study is done for p-type and n-type poly-Si piezoresistive pressure sensors using COMSOL Multiphysics simulation and analytical modeling. The 3D structure of the sensor is modelled with a cantilever beam as a mechanical structure. The Si material is used for the mechanical structure, and a thin SiO_2 layer is used as an insulator between the Si and the sensing layer. Electrodes are placed at the fixed and free ends of the poly-Si of the sensor. Simulations are conducted for the applied pressure ranging from 0 to 100 kPa, and the simulated output resistance is compared with analytical values. A comparative study based on key performance, i.e., sensitivity, polarity, linearity, and output span, of the proposed piezoresistive pressure sensors is conducted.

2. Related Works

The sensitivity, polarity, linearity, and output span of MEMS piezoresistive pressure sensors depend on material properties and device structure. In a semiconductor-based piezoresistive pressure sensor, the change in resistance under applied pressure not only depends on geometric deformation but also on variations in carrier mobility, carrier concentration, and the material's piezoresistive coefficients [2, 8]. Furthermore, the distinct longitudinal piezoresistive coefficients (π_l) of p-type and n-type Si result in opposite sensitivity polarities and different strain responses [9].

In poly-Si, charge carriers move more slowly than in crystalline Silicon because they get scattered more at the edges of tiny grains in the material. Research has shown that poly-Si can be up to ten times more resistant than single-crystalline Si, despite having the same doping concentration [10, 11]. This is because the movement of the majority charge carrier in poly-Si is three to ten times slower than that of crystalline Si on the same doping concentration and temperature. When stress is applied to poly-Si, it changes the structure, which affects both the carrier mobility and the grain boundaries.

This change led to the change in resistivity of the poly-Si under stress, which is the operating principle of the piezoresistive pressure sensor [12]. Studies show that in p-type poly-Si nanofilms, the gauge factor increases with doping concentration up to an optimum level and then decreases. At the same time, low-doped films exhibit greater nonlinearity due to grain-boundary traps [13]. Hence, doping level, carrier type, and microstructure directly influence sensor sensitivity and linearity.

The sensitivity can be enhanced by placing piezoresistive sensing material in high-stress regions of the device structure and using thin membranes or nanowire structures to amplify the strain [14]. However, excessive deflection often leads to nonlinear stress distribution, compromising linearity and output span [15]. Achieving both high sensitivity and good linearity thus requires a balanced approach involving careful control of doping concentration, geometry, and stress distribution. The analysis method can be performed using analytical Modeling and COMSOL simulation.

In recent studies, the performance of the sensors has been improved by using different materials and design innovations. Ultra-thin Silicon-On-Insulator (SOI) -based sensors achieved high sensitivity (34.22 mV/V) and excellent linearity (–0.341%) through precise etching and surface refinement [16]. Flexible porous sensors integrating electron tunneling effects maintained linearity within 7.9% marginal error across pressure ranges [17].

High-temperature p-type SOI sensors exhibited 11.94 mV/V/MPa sensitivity with only 0.99% nonlinearity due to thermal drift compensation [18]. FEM-based optimization of SOI sensors identified low doping and optimal resistor placement as key to maximizing sensitivity (14.65 mV/V/MPa) [19], while Polysilicon-On-Insulator (PSOI) sensors achieved c/bar/mA sensitivity and stable output under 200 mbar [20]. Despite such progress, few studies directly compare p-type and n-type poly-Si sensors under identical conditions.

This present work fills this gap by using both analytical Modeling and COMSOL simulation to examine the performance of p-type poly-Si and n-type poly-Si sensors. The key performance parameters used in this study are sensitivity, polarity, linearity, and output span of the proposed sensor.

3. Analytical Model

This analytical model has two main steps. They are a mechanical model and an electrical model. In mechanical Modeling, the stress produced above the Surface of the piezoresistive material is calculated for the external input pressure. In electric Modeling, the change in output resistance due to the change in induced stress is calculated. Finally, the sensitivity of the piezoresistive-based sensor is calculated for the externally applied pressure.

3.1. Mechanical Modeling

In this study, a cantilever structure is used to design a poly-Si piezoresistive pressure sensor for sensing the pressure. This cantilever structure serves as the main mechanical structure of the sensor. The sizes of the cantilever are Length (l), Breadth (w), and Height (h), which are very important parameters for determining the mechanical deflection and

stress for the applied structure. The model structure of the sensor is shown in Figure 1.

Fig. 1 Block diagram of the sensor

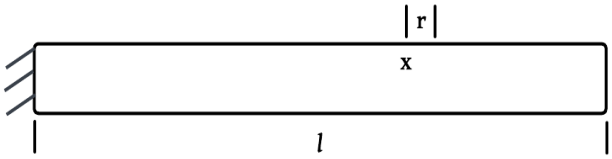

Fig. 2 Cantilever structure for moment calculation

For calculating the stress of the cantilever for the applied pressure, the conservation of moment equation (equilibrium of moments) of the cantilever is considered. The mathematical expression of the equation is as follows [21-23]:

$$-EI\frac{\partial^2 v(x)}{\partial x^2} = Plwx - M_0 - \int_0^x \frac{Plw}{l}(x-r)dr \quad (1)$$

Where M_0 is the moment, E is the Young's modulus, $v(x)$ is the deflection, and I is the moment of inertia, x is any position taken in the length of the cantilever, r is a slight shifting from the x position, P is the applied pressure,

The value of M_o and I is given as follows:

$$M_0 = \frac{Fl}{2} \quad (2)$$

$$I = \frac{h^3 w}{12} \quad (3)$$

After substitution, the value of M_o and I in Equation (1), and differentiating the equation, it can be written as follows:

$$\frac{\partial^2 v(x)}{\partial x^2} = \frac{6}{Elwh^3}(Pwl^3 + Pwlx^2 - 2Pwl^2x) \quad (4)$$

The stress σ(x) function in terms of deflection can be given by Equation (4).

$$\sigma(x) = -Ez\frac{\partial^2 v(x)}{\partial x^2} \quad (5)$$

Where z is the distance of the Surface from the natural point.

After rearranging Equation (4), the stress function of the cantilever is achieved. The stress function of the cantilever is as follows:

$$\sigma(x) = -z\frac{6P}{h^3}(l^2 + x^2 - 2xl) \quad (6)$$

To find the maximum stress of the cantilever, considering the pressure and height are constant, then the term inside the bracket should be maximum. The maximum value of this term is l^2. Now, the maximum stress equation of the cantilever is as follows:

$$\sigma(x)\frac{6P^2}{h^3}_{max} \quad (7)$$

3.2. Electrical Modeling

The resistance R_0 of a semiconductor having a doping concentration of n and carrier mobility μ is given as follows:

$$R_0 = \frac{1}{qnu_n}\frac{l_s}{w_s h_s} \quad (8)$$

Where, l_s is the length of the piezoresistive material, w_s is the width of the piezoresistive material, and h_s is the thickness of the piezoresistive material.

Now, the change in the resistance of the piezoresistive material with piezoresistive coefficient π_l is given as follows:

$$\delta R = \pi_l \sigma(x) R_0 \quad (9)$$

After putting the values of R_0 and σ(x) in Equation (9). The equation of change in resistance can be written as follows:

$$\delta R = -\pi_l z\frac{6P}{h^3}(l^2 + x^2 - 2xl)\frac{1}{qnu_n}\frac{l_s}{w_s h_s} \quad (10)$$

The maximum change in resistance is calculated by the following equation:

$$\delta R = -\pi_l z\frac{6Pl^2}{h^3}\frac{1}{qnu_n}\frac{l_s}{w_s h_s} \quad (11)$$

Finally, the sensitivity of the sensor is calculated by the following equation:

$$\delta R = -\pi_l z\frac{6}{h^3}(l^2 + x^2 - 2xl)\frac{1}{qnu_n}\frac{l_s}{w_s h_s} \quad (12)$$

The maximum sensitivity of the sensor can be calculated by the following equation:

$$\delta R = -\pi_l z\frac{6l^2}{h^3}\frac{1}{qnu_n}\frac{l_s}{w_s h_s} \quad (13)$$

From the above equations, the change in output resistance of the semiconductor-based piezoresistive pressure sensor is determined by the piezoresistive coefficient, distance of the plain from the natural plain, length and height of the cantilever, length, height, and width of the piezoresistive sensing material, doping concentration, and carrier mobility of the materials. The sensitivity is calculated by the ratio of the change in output resistance to the externally applied pressure. So, the factors influencing the sensitivity of the sensor are the same as the factors that affect the change in output resistance.

4. Simulation

The COMSOL Multiphysics simulator is used for the Simulation of the proposed model of the piezoresistive p-type and n-type poly-Si-based pressure sensor by keeping the same structure and dimension for both the sensors. The proposed model of the sensor designed in COMSOL is shown in Figure 3. In this model, the lower block is Silicon, which acts as the main mechanical structure. The middle block is the SiO_2, which acts as an insulator. The above layer is the sensing layer, i.e., n-type or p-type poly-Si. The dimensions of these blocks are tabulated in Table 1. After the model is designed, the various input boundaries, such as ground, electrodes, fixed constraints, and pressure, are applied in the physics section of the COMSOL Multiphysics.

Table 1. Dimensions of the layers in the sensor

Layers Material	Length (µm)	Width (µm)	Height (µm)
Si	200	40	20
SiO2	200	40	2
n-type poly-Si	40	40	5

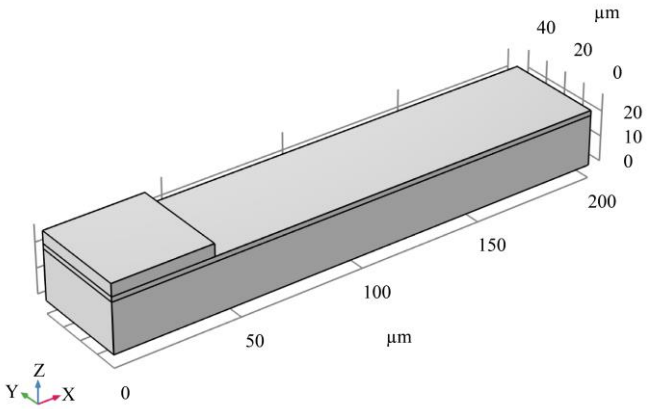

Fig. 3 Proposed sensor model in COMSOL multiphysics simulator

After configuring all the input parameters, the model is meshed with a tetrahedral shape with a finer size. The model of the sensor after meshing is shown in Figure 4.

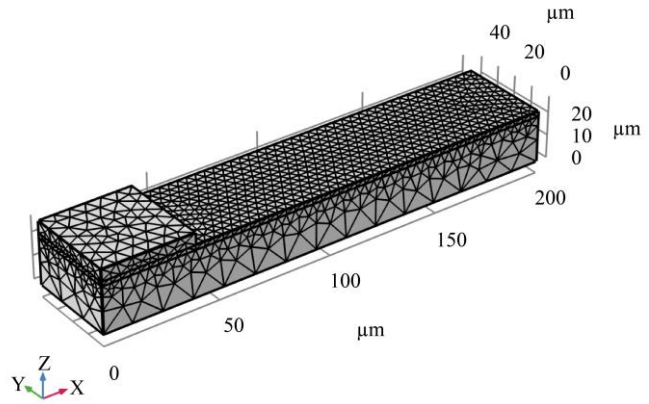

Fig. 4 Meshing of the proposed sensor model

After meshing, the simulations are performed for the applied pressure ranging from 0 kPa to 100 kPa with a step size of 10 kPa. The simulation output of the n-type poly-Si piezoresistive pressure sensor, showing the gradient of electric potential on the Surface of the sensing layer, is shown in Figure 5, and the graph of change in resistance of the n-type polysilicon piezoresistive pressure sensor is shown in Figure 6.

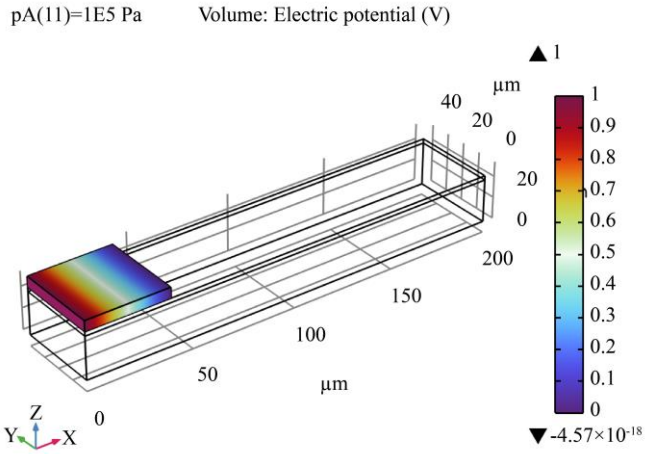

Fig. 5 Gradient of electric potential on the surface of n-type polysilicon piezoresistive layer

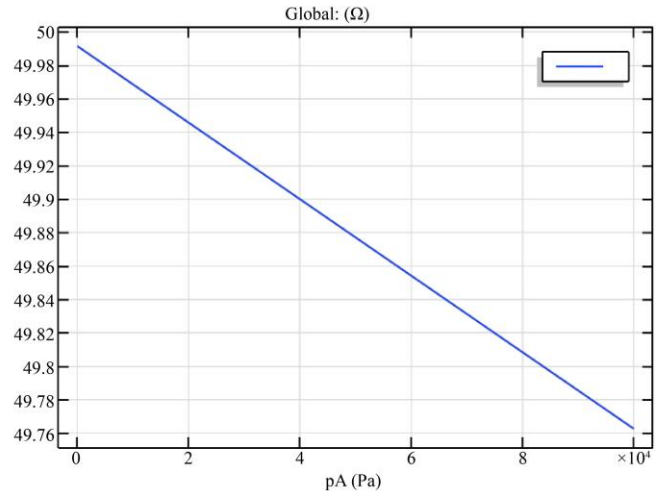

Fig. 6 Change in resistance with change in applied pressure for n-type polysilicon piezoresistive-based sensor

From Figure 5, it is observed that the electric potential is gradually decreasing from the fixed side electrode, which has a 1 V supply, toward the electrode at the free end, which is grounded. So, there is a potential gradient, which means current is flowing through this layer. From Figure 6, it is observed that the resistance decreases with an increase in input pressure.

Similarly, Figure 7 shows the simulation output of the p-type poly-Si piezoresistive pressure sensor showing the

gradient of electric potential, which also decreases from the fixed end toward the free end. It means the current is following through this sensing material. Figure 8 shows the simulated output resistance with respect to applied pressure. It is observed that the resistance increases with an increase in applied pressure.

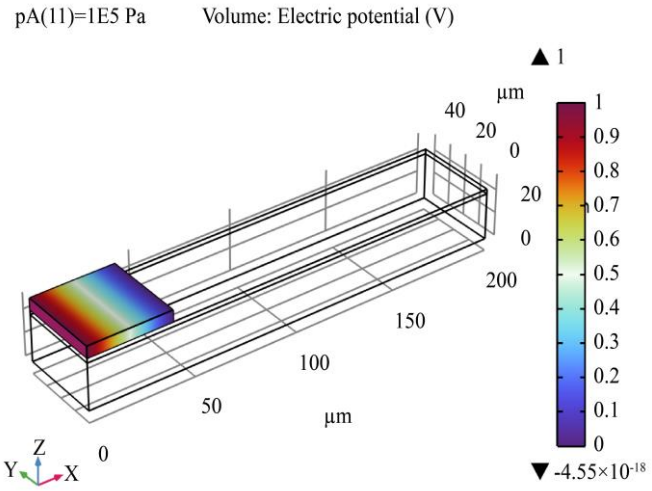

Fig. 7 Gradient of electric potential on the surface of p-type polysilicon piezoresistive layer

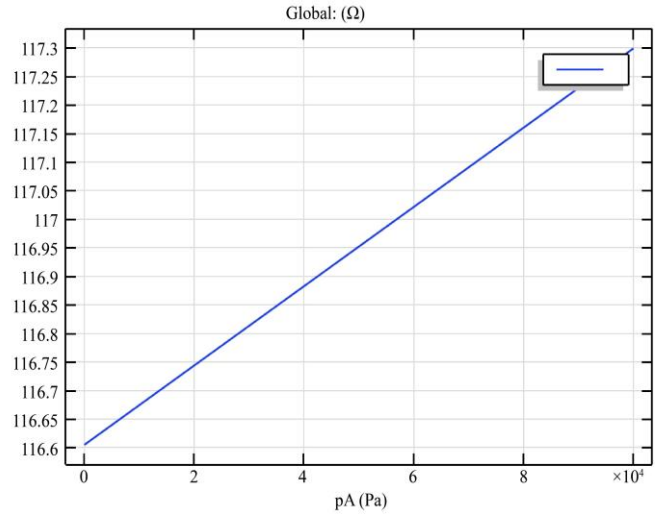

Fig. 8 Change in resistance with change in applied pressure for p-type polysilicon piezoresistive-based sensor

From Figures 6 and 8, it is observed that the resistance is decreasing with an increase in applied pressure for the n-type poly-Si piezoresistive pressure sensor, but the resistance is increasing with an increase in applied pressure for the p-type poly-Si piezoresistive pressure sensor.

5. Results and Discussion

After the Simulation, a comparative study is done for the simulated output and analytical output for the n-type and p-type poly-Si piezoresistive pressure sensor.

Table 2. A comparative study of simulated and analytical output for n-type poly-Si piezoresistive pressure sensor

Applied Pressure [kPa]	Simulated Resistance (Ω)	Analytical Resistance (Ω)
0	49.992	50.000
10	49.969	49.977
20	49.946	49.954
30	49.923	49.931
40	49.900	49.908
50	49.877	49.885
60	49.854	49.862
70	49.831	49.839
80	49.808	49.815
90	49.786	49.792
100	49.763	49.769

Table 2 is the comparative study of simulated output values and analytical values. From this table, it is observed that the simulated output and the analytical values of n-type poly-Si piezoresistive pressure sensors decrease with an increase in applied pressure. The difference between Simulation and analytical values is minimal, and the difference between the successive values of simulated and calculated values is 0.023 Ω in both cases. This indicates that the analytical model is highly accurate and can reliably predict the behavior of the n-type poly-Si piezoresistive pressure sensor without complex simulations. The output resistance is also highly linear with the applied pressure, but with negative slope polarity. The output span of the n-type poly-Si piezoresistive pressure sensor for the externally input pressure ranging from 0 to 10 kPa, simulated and calculated values are 229 mΩ and 231 mΩ.

Table 3. A comparative study of simulated and analytical output for p-type poly-si piezoresistive pressure sensor

Applied Pressure [kPa]	Simulated Resistance (Ω)	Analytical Resistance (Ω)
0	116.60	125.00
10	116.67	125.08
20	116.74	125.16
30	116.81	125.25
40	116.88	125.33
50	116.95	125.42
60	117.02	125.50
70	117.09	125.59
80	117.16	125.67
90	117.23	125.76
100	117.30	125.84

Again, for a p-type poly-Si piezoresistive pressure sensor, a comparative table is shown in Table 3 for simulated output and analytical values for the applied pressure range from 0 to 100 kPa. From Table 3, the analytical values are slightly

higher than the simulated values, but it is observed that the simulated output values and analytical values vary linearly with a positive slope. The slope of simulated values is 0.007 Ω/kPa, while the slope of the analytical values is 0.0084 Ω/kPa with positive polarity. These two slopes are very close to each other. This shows that the analytical model is highly accurate and can reliably predict the behavior of the p-type poly-Si piezoresistive pressure sensor without complex simulations. The output span of the p-type poly-Si piezoresistive pressure sensor for the externally input pressure ranging from 0 to 10 kPa, simulated and calculated values are 700 mΩ and 840 mΩ.

6. Conclusion

This study presents a comparative analysis of n-type and p-type poly-Si piezoresistive pressure sensors using COMSOL Multiphysics simulations and validated with the analytical models. The results show that the n-type poly-Si pressure sensor exhibits a decrease in resistance with increasing pressure. But the p-type poly-Si sensor increases its resistance with an increase in input pressure. The proposed analytical model accurately predicts the resistance changes for the n-type and p-type poly-Si piezoresistive pressure sensor. This means that the analytical model can be used for optimization of the sensor without complex Simulation. The slopes of the output of p-type poly-Si and n-type poly-Si piezoresistive pressure sensors are positive and negative, respectively. This comparative study aims to understand the n-type versus p-type poly-Si behaviour, which will help in material selection. The various factor that influences the sensitivity are doping concentration, majority charge mobility, distance from the neutral point, piezoresistive coefficient, thickness, and length of the cantilever, and dimension of the piezoresistive sensing layer. The sensitivity of the simulated and analytical models for p-type poly-Si piezoresistive pressure sensors is 7.0 mΩ/kPa and 8.4 mΩ/kPa, respectively. The sensitivity of the simulated and analytical models for n-type poly-Si piezoresistive pressure sensors is -2.29 mΩ/kPa and -2.31 mΩ/kPa, respectively. The sensitivity of the p-type poly-Si piezoresistive pressure sensors is higher than that of the n-type poly-Si piezoresistive pressure sensors.

References

[1] Peishuai Song et al., "Recent Progress of Miniature MEMS Pressure Sensors," *Micromachines*, vol. 11, no. 1, pp. 1-38, 2020. [CrossRef] [Google Scholar] [Publisher Link]

[2] A. Alvin Barlian et al., "Review: Semiconductor Piezoresistance for Microsystems," *Proceedings of the IEEE*, vol. 97, no. 3, pp. 513-552, 2009. [CrossRef] [Google Scholar] [Publisher Link]

[3] William Chiappim et al., "The Status and Perspectives of Nanostructured Materials and Fabrication Processes for Wearable Piezoresistive Sensors," *Microsystem Technologies*, vol. 28, pp. 1561-1580, 2022. [CrossRef] [Google Scholar] [Publisher Link]

[4] Xudong Fang et al., "Pressure Sensors Based on the Third-Generation Semiconductor Silicon Carbide: A Comprehensive Review," *Engineering*, vol. 52, pp. 183-203, 2025. [CrossRef] [Google Scholar] [Publisher Link]

[5] A.S. Fiorillo, C.D. Critello, and S.A. Pullano, "Theory, Technology and Applications of Piezoresistive Sensors: A Review," *Sensors and Actuators A: Physical*, vol. 281, pp. 156-175, 2018. [CrossRef] [Google Scholar] [Publisher Link]

[6] Anurag Zope, and Sheng-Shian Li, "CMOS-MEMS Thermal-Piezoresistive Resonators and Oscillators for Sensors," *Frontiers in Mechanical Engineering*, vol. 8, pp. 1-13, 2022. [CrossRef] [Google Scholar] [Publisher Link]

[7] Ashish Kumar et al., "MEMS-based Piezoresistive and Capacitive Microphones: A Review on Materials and Methods," *Materials Science in Semiconductor Processing*, vol. 169, 2024. [CrossRef] [Google Scholar] [Publisher Link]

[8] A.C.H. Rowe, "Piezoresistance in Silicon and its Nanostructures," *Journal of Materials Research*, vol. 29, pp. 731-744, 2014. [CrossRef] [Google Scholar] [Publisher Link]

[9] Hideo Muro, Takeshi Mitamura, and Shigeyuki Kiyota, "Determination of Electrical Properties of n-Type and p-Type Polycrystalline Silicon Thin Films as Sensor Materials," *Sensors and Materials*, vol. 18, no. 8, pp. 433-444, 2006. [Google Scholar] [Publisher Link]

[10] Mojtaba Haghgoo, Reza Ansari, and Saeid Sahmani, "Influence of Nanomaterial Parameters on the Thermoresistivity and Electrical Conductivity of Hybrid Conglomerated CNT/GNP Piezoresistive Polymer Strain Sensors," *Materials Chemistry and Physics*, vol. 344, 2025. [CrossRef] [Google Scholar] [Publisher Link]

[11] Kuan-Ting Chen et al., "Mobility Model based on Piezoresistance Coefficients for Ge 3D Transistor," *Solid State Electronics Letters*, vol. 1, no. 2, pp. 92-97, 2019. [CrossRef] [Google Scholar] [Publisher Link]

[12] M.R. Murti, and K.V. Reddy, "Grain Boundary Effects on the Carrier Mobility of Polysilicon," *Physica Status Solidi (a)*, vol. 119, no. 1, pp. 237-240, 1990. [CrossRef] [Google Scholar] [Publisher Link]

[13] Mikael Santonen et al., "A Detailed Examination of Polysilicon Resistivity Incorporating the Grain Size Distribution," *IEEE Transactions on Electron Devices*, vol. 72, no. 3, pp. 1184-1190, 2025. [CrossRef] [Google Scholar] [Publisher Link]

[14] Priyanshu Verma, Deepak Punetha, and Saurabh Kumar Pandey, "Sensitivity Optimization of MEMS Based Piezoresistive Pressure Sensor for Harsh Environment," *Silicon*, vol. 12, pp. 2663-2671, 2020. [CrossRef] [Google Scholar] [Publisher Link]

[15] Chen Zhou et al., "Effect of Internal Stress on Nonlinearity and Sensitivity of a Pressure Sensor with SiN Composite Diaphragm," *Physics Letters A*, vol. 381, no. 4, pp. 284-291, 2017. [CrossRef] [Google Scholar] [Publisher Link]

[16] Jun-Hwan Choi, and Jung-Sik Kim, "Design and Fabrication of Ultrathin Silicon-based Strain Gauges for Piezoresistive Pressure Sensor," *Current Applied Physics*, vol. 69, pp. 28-35, 2025. [CrossRef] [Google Scholar] [Publisher Link]

[17] Qing Ma, Ding-Yi Xiao, and Yu-Xin Xie, "Multi-scale Modeling of Flexible Piezoresistive Porous Sensors," *European Journal of Mechanics - A/Solids*, vol. 112, pp. 1-11, 2025. [CrossRef] [Google Scholar] [Publisher Link]

[18] Mao Zhou et al., "Design, Fabrication, and Thermal Zero Drift Compensation of a SOI Pressure Sensor for High Temperature Applications," *Sensors and Actuators A: Physical*, vol. 382, 2025. [CrossRef] [Google Scholar] [Publisher Link]

[19] Zhong Jin et al., "Research on Sensitivity Simulation and Optimization of SOI Pressure-Sensitive Chip," *Sensor Review*, vol. 45, no. 6, pp. 801-809, 2025. [CrossRef] [Google Scholar] [Publisher Link]

[20] C. Malhaire, and D. Barbier, "Design of a Polysilicon-on-Insulator Pressure Sensor with Original Polysilicon Layout for Harsh Environment," *Thin Solid Films*, vol. 427, no. 1-2, pp. 362-366, 2003. [CrossRef] [Google Scholar] [Publisher Link]

[21] James M. Gere, and Stephen Timoshenko, *Mechanics of Materials*, PWS Publishing Company, pp. 1-912, 1997. [Google Scholar] [Publisher Link]

[22] Stephen D. Senturia, *Microsystem Design*, Kluwer Academic, pp. 1-689, 2001. [Google Scholar] [Publisher Link]

[23] Minhang Bao, *Analysis and Design Principles of MEMS Devices*, 1st ed., Elsevier, 2005. [CrossRef] [Google Scholar] [Publisher Link]